

Mathematical Modeling And Numerical Simulation of Dropwise Condensation on an Inclined Circular Tube

Hamid Reza Talesh Bahrami¹, Hamid Saffari¹

ABSTRACT: Dropwise condensation can improve heat transfer process and, consequently, leads to considerable reduction in size and weight of condensers as well as improvement in the dehumidification process in many applications, especially in civil transport aircraft. It can also be used as an efficient cooling tool for electronics and electrical systems in aircraft engineering and aerospace technology. In this paper, the stable dropwise condensation on an inclined tube is mathematically analyzed. To do this, the population of small droplets is estimated by population balance theory while an empirical correlation is used for large droplets. To calculate heat transfer across each droplet, sum of temperature drops due to droplet curvature, phase change at droplet-vapor interface, conduction through the droplet and promoter layer, are equated with surface subcooling. The total heat transfer is calculated with the given droplets population and heat transfer through single droplet. Subsequently, effects of various parameters, including surface subcooling, contact angle and contact angle hysteresis on the growth rate, maximum radius of droplet, droplets population, and total heat transfer rate, are investigated. Results show that growth rate and heat flux of small droplets are much higher than those of the larger ones; hence, surface with small droplets is preferred for dropwise condensation purposes. Droplets with low contact angle and contact angle hysteresis have higher heat transfer rates. Increasing the inclination of tube improves heat transfer process to such an extent that vertical tubes have higher heat transfer rate than the horizontal ones. This fact indicates that vertical tubes must be used for designing condensers with dropwise condensation, which is quite the opposite for condensers designed based on filmwise condensation.

KEYWORDS: Dropwise condensation, Mathematical modeling, Air conditioning, Inclined tubes, Contact angle.

INTRODUCTION

Condensation is one of the most important regimes of heat transfer, which plays a significant role in many industries including aerospace engineering, power plants and refrigeration as well as natural phenomena such as fog or rain formation. Condensation process in industrial applications usually occurs on surfaces, which appears as a liquid film (filmwise condensation), droplets (dropwise condensation), or a combination of both. In dropwise condensation on surfaces, small droplets appear on nucleation sites and grow initially by direct condensation from adjacent vapor. Next, when their size becomes notable so that they can contact neighbor droplets, growing process proceeds by coalescing. Large droplets leave the surface by gravity or other shear forces and sweep other droplets in their way. In stable condition, these processes occur repeatedly and a hierarchical process is formed (Sikarwar *et al.* 2013). Dropwise condensation plays 2 paradox roles in many industries. It shows a negative effect on dew formation on airplane windshield (Fayazbakhsh and Bahrami 2013) and vapor trail around airplanes (Goncalvccedil *et al.* 2003; Yamamoto 2003), while it has a positive role in air conditioning of civil transport aircraft. If dropwise condensation is used in the condensers of air conditioning system of an aircraft, it leads to considerable reduction in size and weight of condensers besides improvement in the dehumidification process (Leipertz and Fröba 2008). Dropwise condensation can also be used in the cooling of electronic systems of aerospace industries (O'Callaghan and Babus'Haq 1990). In the following, the positive role of dropwise condensation and enhancement of heat transfer process are addressed.

¹Iran University of Science and Technology – School of Mechanical Engineering – Liquefied Natural Gas Research Laboratory – Tehran/Tehran – Iran.

Author for correspondence: Hamid Saffari | Iran University of Science and Technology – School of Mechanical Engineering – Liquefied Natural Gas Research Laboratory | Narmak | 16846-13114 – Tehran/Tehran – Iran | Email: saffari@iust.ac.ir

Received: Oct. 01, 2016 | **Accepted:** Apr. 22, 2017

Previous studies have shown that dropwise condensation has about one order of magnitude greater heat transfer coefficient than filmwise condensation (Schmidt *et al.* 1930; Rose 2002). Hence, many investigations have experimentally or numerically conducted to the dropwise condensation in recent years (Leipertz and Fröba 2008; Kananeh *et al.* 2010; Sikarwar *et al.* 2012; Reis *et al.* 2016). As an example, McNeil and Burnside (2000) experimentally investigated the performance of both dropwise condensation and filmwise condensation on small tube bundles. Their results show that a durable dropwise condensation can significantly reduce condensers size. Although experimental design of industrial systems is the most reliable approach, it is very expensive especially when many trial and error processes are required. Thus, the development of numerical approaches, which can be used as robust and inexpensive tools for primary or even final design, is important. The earliest theoretical approach for dropwise condensation is proposed by LeFevre and Rose (1966). Consequently, many efforts have been made to improve theoretical approaches (Glicksman and Hunt 1972; Wen and Jer 1976; Maa 1978; Abu-Orabi 1998; Wu *et al.* 2001; Sun *et al.* 2007). Sikarwar *et al.* (2011) conducted an experimental study on the dropwise condensation underneath chemically textured surfaces, while they numerically simulated the same conditions. Battoo *et al.* (2010) presented a numerical simulation for dropwise condensation on inclined surfaces. They investigated the effects of various parameters including contact angle, inclination, contact angle hysteresis, and saturation temperature on dropwise condensation. Wu *et al.* (2001) conducted a numerical simulation on the dropwise condensation on various substrates to discover effects of surface conductivity. They showed that heat transfer of dropwise condensation declines with increasing substrate thermal conductivity. Enright *et al.* (2014) reviewed recent experimental and theoretical studies on the dropwise condensation on micro- and nano-structured surfaces.

The literature shows that very little theoretical studies have been published on dropwise condensation on horizontal or inclined tubes although many experimental ones have been reported (Miljkovic and Wang 2013; Preston 2014). Hosokawa *et al.* (1995) studied single droplets departure heat transfer characteristics in dropwise condensation on an inclined tube. They show that heat transfer coefficient is maximal at inclination angle of 30°. Hu and Tang (2014) presented a theoretical model for dropwise condensation on

a horizontal tube. They investigated the effects of various parameters including subcooling temperature and contact angle on both single droplet and overall heat transfer process.

Although numerous research studies have been published on numerical simulation of filmwise condensation inside or outside of tubes (Ji *et al.* 2009; Palen *et al.* 1979; Yun *et al.* 2016), there are very few studies reported in the literature on total heat transfer behavior of dropwise condensation on inclined tubes. According to much higher thermal performance of dropwise condensation compared to filmwise condensation and recent advances in achieving durable dropwise condensation, it is necessary to develop more reliable and robust numerical tools to simulate dropwise condensation.

In this study, a numerical model for dropwise condensation on an inclined tube is developed based on the method presented by LeFevre and Rose (1966). Accordingly, small droplets population is estimated with population balance theory and large droplets population is estimated with the correlation proposed by LeFevre and Rose (1966). Single droplet heat transfer is derived according to contact angle, contact angle hysteresis, tube inclination, nucleation site density, and promoter layer thickness. With the given single droplet heat transfer rate and droplets population, the overall heat transfer rate is calculated. In the following, the effects of various parameters on single droplet behavior or overall heat transfer are investigated.

HEAT TRANSFER MODEL

It is assumed that condensing droplets grow on the nucleation sites (active area) and other sections of the substrate are inactive. Heat transfer through these inactive surfaces is neglected because vapor loses its latent heat at active sites while losing its sensible heat in inactive areas.

The heat flow between the vapor and surface through a single droplet must overcome some thermal resistances, as shown in Fig. 1, where R_d , R_c , R_i and R_{hc} are, respectively, droplet conduction thermal resistance, droplet curvature thermal resistance, liquid-vapor interfacial thermal resistance and hydrophobic coating thermal resistance, all in k/W. Thermal resistances in dropwise condensation modeling are usually expressed as temperature drop, which will be extracted in the following sections.

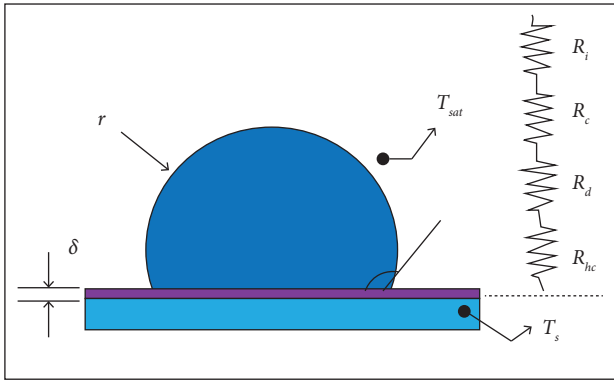


Figure 1. Sketch of necessary parameters and heat transfer resistances between the surface and the vapor through a droplet.

TEMPERATURE DROP OF DROPLET SURFACE CURVATURE

Droplet surface curvature results in higher vapor pressure of the droplet. Temperature drop through the droplet surface (K) is calculated by assuming a continuous Gibbs function across the interface, ideal-gas behavior of the vapor, small and constant specific volume of fluid, and using Clausius-Clapeyron equation along with Young-Laplace equation as follows (Thome 2015):

$$\Delta T_c = \frac{2T_{sat}\sigma}{rh_{fg}\rho_w} \quad (1)$$

where T_{sat} is the saturation temperature (K); σ is the condensate surface tension (N/m); r is the droplet radius (m; Fig. 1); h_{fg} is the latent heat (J/kg); ρ_w is the condensate density (kg/m^3).

The minimum droplet radius (r_{min} ; m) for the smallest stable droplet is calculated by considering thermodynamic constraints. Molecule clusters with a size smaller than this limit are unstable and decompose; r_{min} is written as (Carey 2007):

$$r_{min} = \frac{2T_{sat}\sigma}{h_{fg}\rho_w\Delta T} \quad (2)$$

where ΔT is the subcooling temperature.

Combining Eqs. 1 and 2, the temperature drop due to droplet surface curvature can be simplified as:

$$\Delta T_C = \frac{r_{min}}{r} \Delta T \quad (3)$$

According to Eq. 3, smaller droplets have higher ΔT_c .

Temperature drop of vapor-liquid interfacial resistance

Only some fraction of vapor molecules colliding with the droplet surface is absorbed by the liquid phase. This non-ideal process imposes an extra resistance through the heat transfer route as:

$$\Delta T_i = \frac{q_d}{2\pi r^2 h_i (1 - \cos \theta)} \quad (4)$$

where q_d is the heat transfer rate through the droplet (W); θ is the contact angle (deg; Fig. 1); h_i is the interfacial heat transfer coefficient between the vapor and liquid (W/mK), which is derived based on the Kinetic Theory of Gases (Schrage 1953; Rohsenow 1972):

$$h_i = \frac{2\varepsilon}{2 - \varepsilon} \frac{1}{\sqrt{2\pi R_g T_s}} \frac{h_{fg}^2}{v_g T_s} \quad (5)$$

where R_g , h_{fg} , T_s and v_g are gas constant, latent heat of condensation, saturation temperature and specific volume of the vapor, respectively; ε , which is called condensation coefficient (Wen and Jer 1976) or accommodation coefficient (Liu and Cheng 2015a), is the ratio of molecules absorbed by the liquid phase from the total colliding molecules to the liquid surface; h_i depends on the vapor pressure ranging from 0.383 to 15.7 MW/m²K for pressure from 0.01 to 1.0 atm (Tanasawa 1991).

TEMPERATURE DROP OF CONDUCTION THROUGH DROPLET

The heat flux transferred to the liquid surface must conduct through the droplet to reach the condenser surface, which causes the following temperature drop (Kim and Kim 2011):

$$\Delta T_d = \frac{q_d \theta}{4\pi r k_w \sin \theta} \quad (6)$$

where k_w is the water thermal conductivity (W/mK).

The value of ΔT_d depends highly on the droplet contact angle. When contact angle reaches to 180°, ΔT_d goes up to very large values. This means that surfaces with very large contact angle are not proper for condensation purposes. On

the other hand, droplets with larger radius (with $\theta < 180^\circ$) have lower temperature drop with respect to smaller droplets with the same contact angle. This is because larger droplets have greater interface with the condenser surface.

TEMPERATURE DROP OF PROMOTER LAYER

The surfaces of condensers are usually made of industrial metals such as steel, aluminum, or copper, which are hydrophilic and have high surface energy. Therefore, some hydrophobic materials are used as coating to enhance surface hydrophobicity. This coating causes the following temperature drop (Miljkovic *et al.* 2012):

$$\Delta T_{hc} = \frac{q_d \delta}{\pi r^2 k_{coat} (\sin \theta)^2} \tag{7}$$

where δ and k_{coat} are the promoter layer thickness and conductivity, respectively.

This temperature drop adversely depends on the contact angle. Due to smaller base area, droplets with larger contact angle have smaller ΔT_{hc} .

SINGLE DROPLET GROWTH RATE

Equating the sum of all temperature drops, Eqs. 1 to 7, with subcooling temperature, ΔT , the heat transfer through a single droplet is evaluated as follows:

$$q_d = \frac{\Delta T \pi r^2 (1 - \frac{r_{min}}{r})}{\frac{1}{2h_i(1 - \cos \theta)} + \frac{r\theta}{4k_w \sin \theta} + \frac{\delta}{k_{coat} (\sin \theta)^2}} \tag{8}$$

The total heat transfer through a single droplet can also be calculated by considering the droplet phase change rate:

$$q_d = \rho_w h_{fg} \frac{dV}{dt} = \frac{\pi}{3} \rho_w h_{fg} \frac{d}{dt} \left\{ (1 - \cos \theta)^2 \times (2 + \cos \theta) r^3 \right\} \tag{9}$$

where V is the droplet volume; t represents time (s).

Making Eqs. 8 and 9 equivalent, the droplet growth rate (G , m/s), is obtained as:

$$G = \frac{dr}{dt} = \frac{1}{\rho_w h_{fg} (1 - \cos \theta)^2 (2 + \cos \theta)} \times \frac{\Delta T (1 - \frac{r_{min}}{r})}{\frac{1}{2h_i(1 - \cos \theta)} + \frac{r\theta}{4k_w \sin \theta} + \frac{\delta}{k_{coat} (\sin \theta)^2}} \tag{10}$$

Equation 10 can be summarized by introducing the following parameters:

$$A_1 = \frac{\Delta T}{\rho_w h_{fg} (1 - \cos \theta)^2 (2 + \cos \theta)} \tag{11}$$

$$A_2 = \frac{\theta}{4k_w \sin \theta} \tag{12}$$

$$A_3 = \frac{\delta}{k_{coat} (\sin \theta)^2} + \frac{1}{2h_i(1 - \cos \theta)} \tag{13}$$

Then, Eq. 10 is rewritten as:

$$G = A_1 \frac{(1 - \frac{r_{min}}{r})}{A_2 r + A_3} \tag{14}$$

MAXIMUM DROPLET RADIUS

After the birth of a condensing droplet, it first grows with direct condensation and then condenses with neighbor droplets. Along with the growth of the droplet, both surface tension, which adheres it to the surface, and gravity forces (in the absence of other shear forces) increase. When the gravity force overcomes the adhering force, the droplet falls or slides on the surfaces. Surface curvature determines the magnitude of gravity force. A single droplet, which is deposited on an inclined tube and is on the verge of sliding, is schematically shown in Fig. 2.

FIRST METHOD TO DETERMINE THE DROPLET MAXIMUM RADIUS

Initially, it is assumed that the droplet on the verge of sliding is a spherical cap and r_{max} is found by equating gravity and surface tension forces. This method is used by numerous

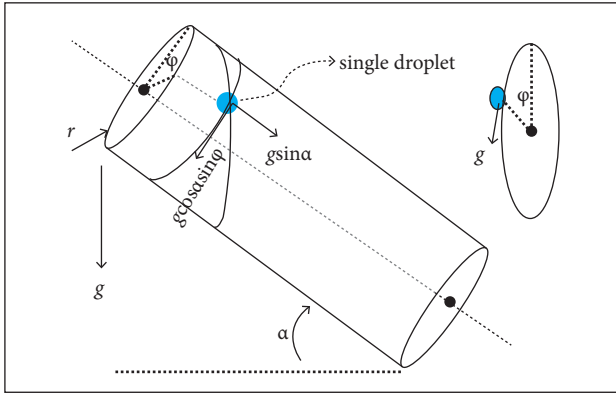


Figure 2. Schematics of gravity forces acting on a droplet on an inclined tube.

researchers in dropwise condensation modeling on inclined surfaces (e.g., Dimitrakopoulos and Higdon 1999; Kim and Kim 2011; Kumar and Yuvaraj 2013; Lee *et al.* 2013; Hu and Tang 2014; Cheng *et al.* 2015; Liu and Cheng 2015b). The maximum radius is evaluated as follows. The gravity force exerted on the droplet is:

$$F_g = (2 - 3\cos\theta + \cos^3\theta) \pi r_{max}^3 \frac{\rho g}{3} \times \sqrt{\cos^2 \alpha \sin^2 \varphi + \sin^2 \alpha} \quad (15)$$

where r_{max} is the maximum droplet radius; g is the acceleration of gravity (m/s²); α is the inclination angle (deg); φ is the peripheral angle (deg).

The surface tension force depending on the droplet shape is (Kim *et al.* 2002):

$$F_\sigma = 2\sigma r_{max} \sin\theta (\cos\theta_r - \cos\theta_a) \quad (16)$$

where θ_r and θ_a are the receding and the advancing angles, respectively.

When a droplet is deposited on an inclined surface, it alters its shape to produce extra surface tension and resists leaving the surface. This reaction appears in the droplet receding and advancing angles.

Making Eqs. 15 and 16 equivalent, r_{max} is found as:

$$r_{max}(\varphi, \alpha) = \left[\frac{6\sigma \sin\theta (\cos\theta_r - \cos\theta_a)}{\pi(2 - 3\cos\theta + \cos^3\theta) \rho g \sqrt{\cos^2 \alpha \sin^2 \varphi + \sin^2 \alpha}} \right]^{1/2} \quad (17)$$

SECOND METHOD TO DETERMINE THE DROPLET MAXIMUM RADIUS

Droplets on inclined surfaces deform and take a shape other than spherical cap. For this reason, receding and advancing angles appear. Some researchers have considered this deformation and shown that the assumption of spherical cap cannot properly estimate droplet volume on inclined surfaces. As an example, ElSherbini and Jacobi (2004, 2006) can be mentioned. However, the relation for volume of droplets on the verge of sliding on inclined surfaces proposed by Dussan (1985) is straightforward and can be simply used considering peripheral inclination:

$$v_{max}(\varphi, \alpha) = \left(\frac{\rho g \sqrt{\cos^2 \alpha \sin^2 \varphi + \sin^2 \alpha}}{\sigma} \right)^{-\frac{3}{2}} \left(\frac{96}{\pi} \right)^{\frac{1}{2}} \times \left((\cos\theta_r - \cos\theta_a)^{\frac{3}{2}} (1 + \cos\theta_a) \right) \times \left(1 - \frac{3}{2} \cos\theta_a + 1/2 \cos^3\theta_a \right) \times \left((\cos\theta_a + 2)^{\frac{3}{2}} (1 - \cos\theta_a)^{9/4} \right)^{-1} \quad (18)$$

The equivalent radius can be derived as:

$$r_{max} = \left(\frac{v_{max}(\varphi, \alpha)}{\pi(2 - 3\cos\theta + \cos^3\theta)} \right)^{\frac{1}{3}} \quad (19)$$

The results are reported for hysteresis angle up to 10 deg in Dussan (1985). In the next sections, both Eqs. 17 and 19 will be used for simulation.

EFFECTIVE RADIUS

Effective radius (r_e, m) is the half of the average distance between nucleation sites given by Wen and Jer (1976), Abu-Orabi (1998), and Kim and Kim (2011):

$$r_e = \sqrt{\frac{1}{4N_s}} \quad (20)$$

where N_s is the density of nucleation sites on the condensing surface (1/m).

Equation 20 is derived based on the assumption that nucleation sites form a square array. The effective radius is a measure that determines when a growing droplet contacts a neighbor droplet.

DROPLET SIZE DISTRIBUTION

After estimating single droplet thermal behavior, droplets size distribution must be established. This distribution determines how many droplets with a specific size exist on the surface in the stable dropwise condensation at every moment. Population balance theory has been used in the literature (Tanaka 1975; Maa 1978; Abu-Orabi 1998; Vemuri and Kim 2006; Kim and Kim 2011) to derive size distribution of small droplets, which mainly grow by direct condensation. Based on this theory, in the stable dropwise condensation, the number of droplet entering a specific droplet radius range is equal with those leaving the range. Assuming a droplet radius range of $r_1 < r < r_2$, the number of droplets that enters this range in the interval Δt is:

$$AG_1 n_1 \Delta t \tag{21}$$

and the number of the droplets that leaves this range is:

$$AG_2 n_2 \Delta t \tag{22}$$

where n is the population density of small droplets growing by direct condensation (m^3).

The number of small droplet swept with larger sliding droplets can be considered as:

$$S \bar{n} \Delta t \Delta r \tag{23}$$

where S is the rate at which the small droplets are swept by falling droplets; \bar{n} is the average population density in the range $r_1 < r < r_2$, and $\delta r = r_2 - r_1$.

Making Eqs. 21 - 23 equivalent as well as Δt and Δr sufficiently close to 0, the population balance theory is reduced to:

$$\frac{dG}{dt} + \frac{n}{\tau} = 0 \tag{24}$$

where τ is the sweeping period ($\tau = A/S$).

Equation 24 is suitable for small droplets growing mainly by direct condensation. However, when the radii of small

droplets exceed the effective radius, they coalesce with neighbor droplets. After this step, droplets mainly grow by coalescence and they are called large droplets. LeFevre and Rose (1966) proposed the following relation for size distribution of large droplets, which have been used in many studies in the literature (e.g., Vemuri and Kim 2006; Hu and Tang 2014; Liu and Cheng 2015a):

$$N(r) = \frac{1}{3\pi r^2 r_{max}(\varphi, \alpha)} \left(\frac{r}{r_{max}(\varphi, \alpha)} \right)^{-2/3} \tag{25}$$

where N is the population density of large droplets (m^3).

Equation 24 is an ordinary differential equation of order one with an exact closed-form solution. Rearranging and integrating Eq. 24, one has:

$$n(r) = \frac{(Gn)_{min}}{G} \exp \left(\frac{A_2}{\tau A_1} \left[\frac{(r - r_{min}^2)}{2} + 2r_{min}(r - r_{min}) + r_{min}^2 \ln(r - r_{min}) \right] + \frac{A_3}{\tau A_1} [r - r_{min} + r_{min} \ln(r - r_{min})] \right) \tag{26}$$

where $(Gn)_{min}$ and τ are unknown terms determined by the following boundary conditions:

$$N(r) = n(r) \quad \text{at } r = r_e \tag{27}$$

and

$$\frac{d(\ln n(r))}{d(\ln r)} = \frac{d(\ln n(r))}{d(\ln r)} = -8/3 \tag{28}$$

which means that the value and slop of small and large droplet distributions are equal at effective radius. Applying boundary conditions, one has:

$$n(r) = \frac{1}{3\pi r_e^3 r_{max}} \left(\frac{r_e}{r_{max}} \right)^{-2/3} \frac{r(r_e - r_{min})}{r - r_{min}} \times \frac{A_2 r + A_3}{A_2 r_e + A_3} \exp(B_1 + B_2) \tag{29}$$

where:

$$B_1 = \frac{A_2}{\tau A_1} \left[\frac{r_e^2 - r^2}{2} + r_{min}(r - r_{min}) - r_{min}^2 \times \ln \left(\frac{r - r_{min}}{r_e - r_{min}} \right) \right] \tag{30}$$

$$B_2 = \frac{A_3}{\tau A_1} \left[r_e - r - r_{min} \ln \left(\frac{r - r_{min}}{r_e - r_{min}} \right) \right] \quad (31)$$

and

$$\tau = \frac{3r_e^2 (A_2 r_e + A_3)^2}{A_1 (11A_2 r_e^2 - 14A_2 r_e r_{min} + 8A_3 r_e - 11A_3 r_{min})} \quad (32)$$

TOTAL HEAT FLUX

With known single droplet heat transfer and droplets distribution, total heat flux can be determined as:

$$q''(\alpha, \theta) = \frac{1}{2\pi} \left[\int_0^{2\pi} \int_{r_{min}}^{r_e} q_d(r, \theta, \varphi, \alpha) n(r, \theta, \varphi, \alpha) dr d\varphi + \int_0^{2\pi} \int_{r_e}^{r_{max}(\theta, \varphi, \alpha)} q_d(r, \theta, \varphi, \alpha) N(r, \theta, \varphi, \alpha) dr d\varphi \right] \quad (33)$$

where: q'' is the heat flux (W/m^2).

NUMERICAL PROCEDURE VALIDATION

To verify the presented procedure, the calculated heat flux is compared with reported experimental results of Peng *et al.* (2015). Nucleation site numbers reported in the literature are in the range of $10^9 < N_s < 10^{13}$ (Vemuri and Kim 2006). The nucleation site number is considered 10^{12} in this comparative study. According to Peng *et al.* (2015), contact angle, advancing and receding angles are 120° , 142° , and 102° , respectively. Effects of non-condensable gases and thermal resistance of hydrophobic promoter layer are neglected. In addition, the simulation is performed in atmospheric conditions. The comparative results are illustrated in Fig. 3. As it can be seen, there is a good agreement between the predicted and the experimental results.

As another example, the current study is compared with the reported experimental results of Vemuri and Kim (2006). They experimentally measured the maximum radius of droplet on the surface, $r_{max} = 1.5$ mm. Therefore, r_{max} is directly put in the code and Eq. 19 is omitted. The simulation is done with nucleation site number of 10^{12} , contact angle of 149° and at atmospheric condition according to Vemuri and Kim (2006).

A good agreement can be seen between the current study and that of Vemuri and Kim (2006), as shown in Fig. 4.

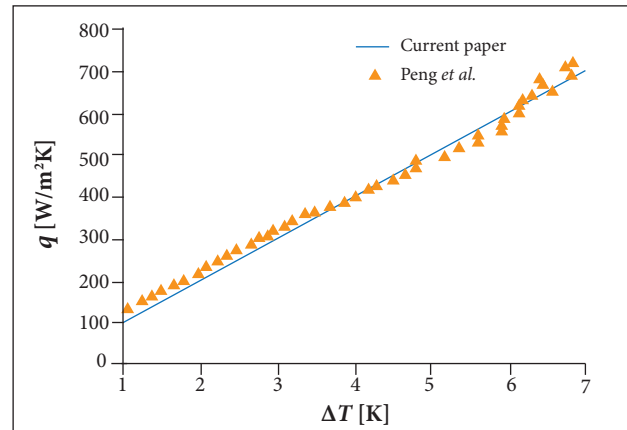


Figure 3. Comparison of the current simulation and that of Peng *et al.* (2015).

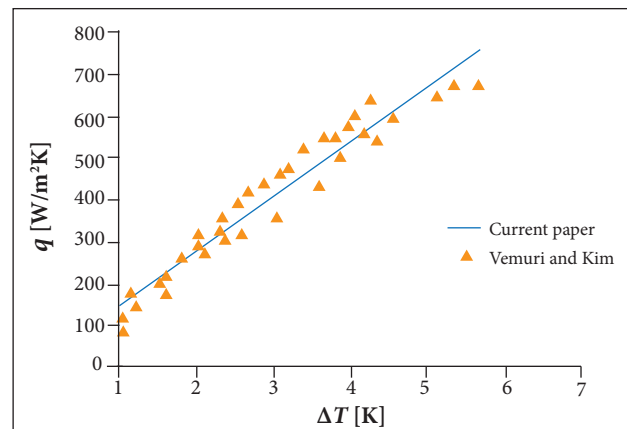


Figure 4. Comparison of the current simulation and that of Vemuri and Kim (2006).

RESULTS AND DISCUSSION

SINGLE DROPLET BEHAVIOR

The variation of different temperature drops is shown in Fig. 5, where $\theta = 120^\circ$, $\Delta\theta = 40^\circ$, $\alpha = 90^\circ$, $\Delta T = 1$ K, and $\delta = 1$ μm ; $\Delta\theta$ is the contact angle hysteresis (deg). All temperature drops are comparable in very small radii while ΔT_d is the prevalent temperature drop in very large droplets. The variation of single droplet heat flux and heat transfer rate are shown in Fig. 6, where $\theta = 120^\circ$, $\Delta\theta = 40^\circ$, $\alpha = 90^\circ$, $\Delta T = 1$ K, and $\delta = 1$ μm . Although larger droplets have higher heat transfer rate, they have low heat flux. It means that surfaces with more small droplets have higher heat transfer rate. Hence, for dropwise condensation

purpose, it is preferred to have surfaces in which small droplets could slide quickly and easily from the surface to more small droplets form.

Variation of thermal resistances with respect to contact angle (CA) is shown in Fig. 7. All thermal resistances increase with contact angle and the thermal resistance curvature is not considerable with respect to other resistances due to vapor-liquid interface. However, all resistances increase with contact angle. For example, it can be roughly said that all resistances increase by 100 times when contact angle is increased from 100° to 160°.

The variation of single droplet growth rate due to direct condensation (Eq. 14) with respect to radius and subcooling temperature is shown in Fig. 8, where $\theta = 120^\circ$, $\Delta\theta = 40^\circ$, $\alpha = 90^\circ$, and $N_s = 10^{12}$ (1/m²). The growth rate of small droplets is higher at greater subcooling. Also, growth rate of large droplets is very low at all subcooling temperatures.

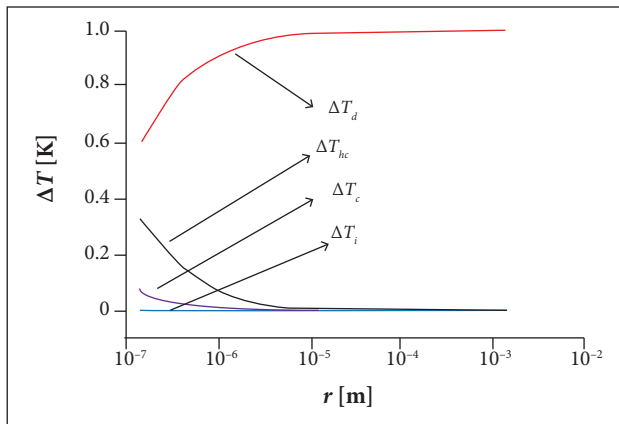


Figure 5. Variation of different temperature drops with respect radius.

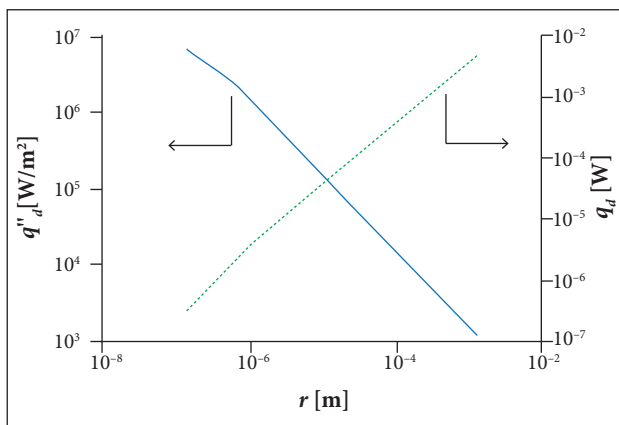


Figure 6. Variation of heat flux and heat transfer rate of a single droplet with respect radius.

The variation of single droplet growth rate with respect to radius and contact angle is illustrated in Fig. 9, where $\Delta T = 5$ K, $\Delta\theta = 40^\circ$, $\alpha = 90^\circ$, and $N_s = 10^{12}$ (1/m²). At the

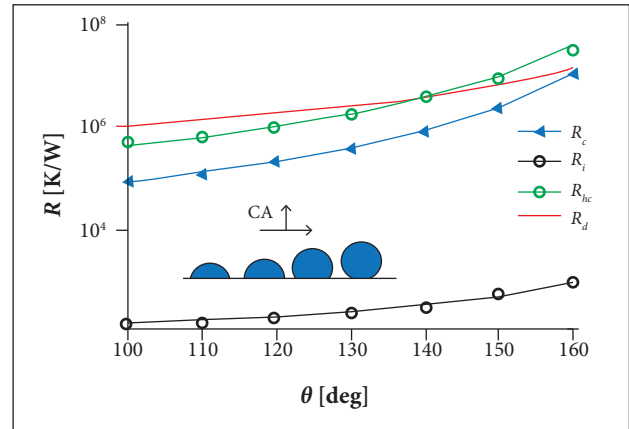


Figure 7. Variation of thermal resistances with contact angle ($r = 1 \mu\text{m}$).

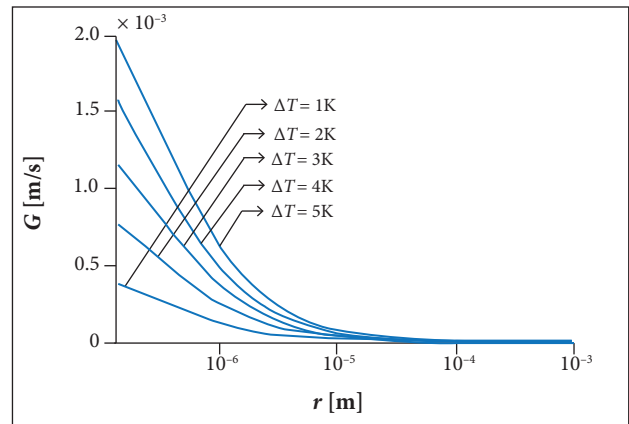


Figure 8. Variation of a droplet growth rate for radius and surface subcooling temperature.

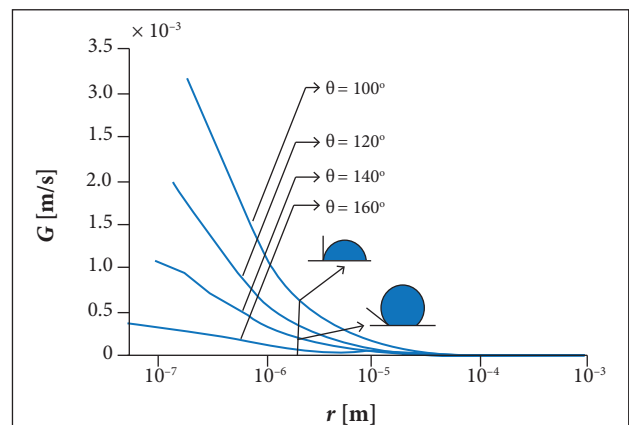


Figure 9. Variation of a droplet growth rate with respect to its radius and contact angle.

same radius, droplets with higher contact angle have lower growth rate. For example, droplets with contact angle of 100° have 6 times higher growth rate than droplets with contact angle of 160° at small radii. This is because droplets with smaller contact angle have larger interface with the surface. On the other hand, droplets with lower contact angle have smaller mobility. Therefore, there is a conflict between droplet mobility and its heat transfer rate.

Previous studies have shown that dropwise condensation is a nucleation phenomenon and that droplets form at the same positions repeatedly (McCormick and Westwater 1965). Assuming that dropwise condensation is a nucleation process, nucleation site number has a significant effect on it. With increasing nucleation sites, the density of small droplets increases and accordingly heat transfer process is improved. Nucleation site number depends on the topography and chemical properties of the surface (Mu *et al.* 2008). However, there is not any comprehensive correlation for estimating nucleation site number on various surfaces. The variation of droplet distribution at various nucleation site numbers is shown in Fig. 10, where $\theta = 120^\circ$, $\Delta T = 10$ K, and $\alpha = 0^\circ$. The nucleation site numbers has a significant effect on small droplets population with radii smaller than effective radius. For radii greater than r_e droplets, the population is independent of nucleation sites number determined from Eq. 25. Very high nucleation site numbers, $N_s > 10^{13}$, lead to high droplets population and small effective radii. These consequences result in droplets coalescence once they nucleate, and filmwise condensation appears. As previous studies have revealed, small nucleation site numbers lead to inaccurate results (Citakoglu and Rose 1969).

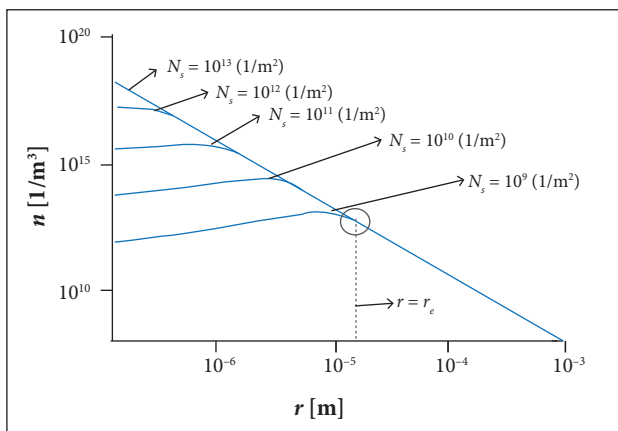


Figure 10. Variation in population of droplets for radius at various numbers of nucleation sites.

Droplet minimum radius (r_{min}) is extracted from thermodynamic minimization. Figure 11 depicts the variation of droplets population with respect to radius at different minimum radii, where $N_s = 10^9$ ($1/m^2$), $\theta_a = 142^\circ$, $\theta_r = 102^\circ$, $\theta = 120^\circ$, $\Delta T = 10$ K, and $\alpha = 0^\circ$. It can be considered that population distributions (except for $1,000r_{min}$) have a bell-like shape where the maximum population is $n = 1.2 \times 10^{13}$ ($1/m^3$) locating at effective radius (here, $r_e = 1.5 \times 10^{-5}$ m). The average radius of droplets is $\bar{r} = 6.6 \times 10^{-4}$ m with variance 1.46×10^{-7} . If the minimum radius is exaggeratedly increased ($1,000r_{min}$), a non-physical condition appears. However, even 100 times increase in minimum radius does not have a considerable effect on droplets population.

The maximum radius variation with respect to hysteresis angle at different inclination angles is depicted in Fig. 12, where $\Delta T = 10$ K and $\theta = 120^\circ$ (Fig. 12a) and $\Delta T = 10$ K, $\theta = 120^\circ$, and $\alpha = 10^\circ$ for the difference of 2 estimates for maximum radius at different hysteresis angles (Fig. 12b). Equation 17 overestimates r_{max} with respect to Eq. 19. Also, the difference of 2 estimations reduces in higher hysteresis angles. In the next sections, Eq. 19 will be used for estimations with hysteresis angle lower than 10° .

The variation of maximum radius with respect to hysteresis angle at different contact angle is depicted in Fig. 13 ($\Delta T = 10$ K). As hysteresis or contact angle increases, the maximum radius increases. The figure shows that if droplet contact angle increases from 2° to 90° , the maximum radius increases 6 times. On the other hand, droplet population distributions are close together in small sliding angles. It should be mentioned that producing surfaces with simulta-

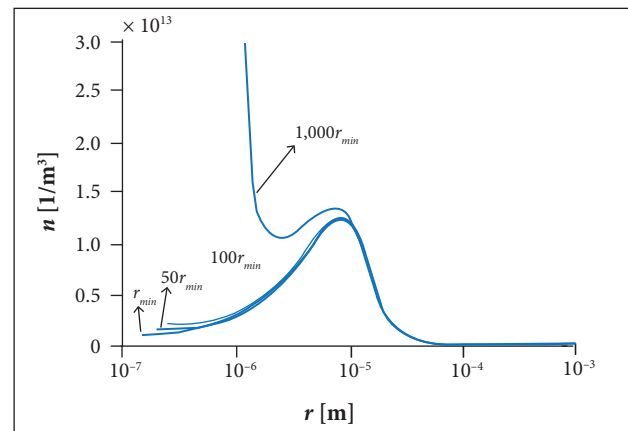


Figure 11. Variation in the number of droplets for radius at various minimum ones.

neous low contact angle and low hysteresis angle is not practically possible (Talesh Bahrami *et al.* 2017). The effect of maximum radius on dropwise condensation will be considered in the next sections.

The variation of maximum droplet radius with respect to peripheral angle at different tube inclinations is shown in

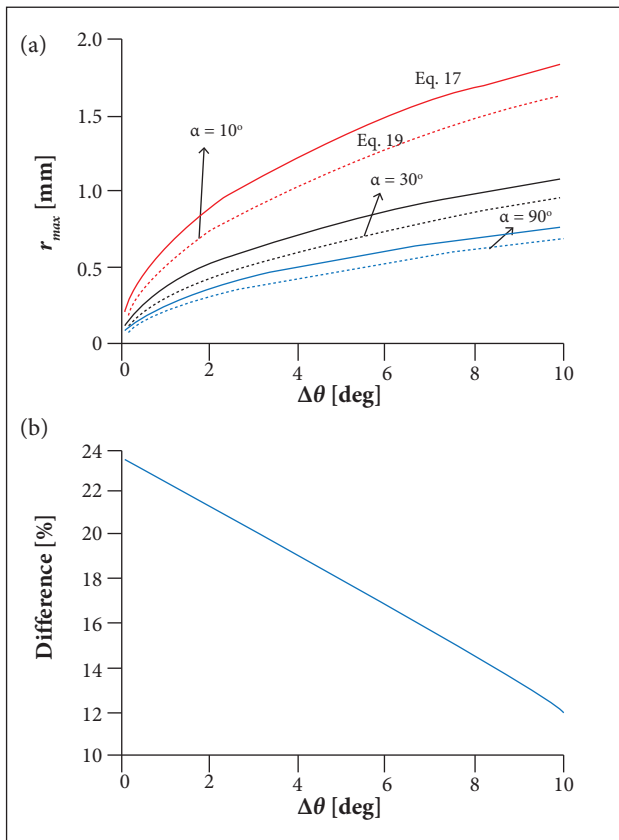


Figure 12. Maximum radius variation for hysteresis angle at different inclination angles.

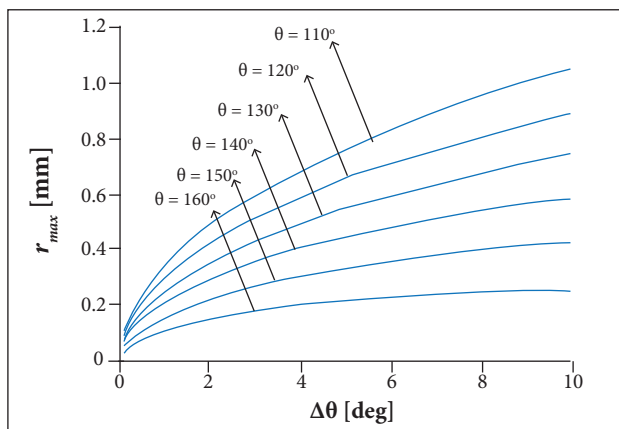


Figure 13. Variation of maximum droplet radius for contact angle hysteresis on a vertical plate.

Fig. 14, where $\Delta T = 10$ K and $\Delta\theta = 10^\circ$. The maximum radius increases with decrease in inclination. This analysis is not valid for horizontal surfaces where due to the absence of a proper sweep mechanism, droplets continuously coalesce together. Finally, a continuous liquid film covers the surface and dropwise condensation assumption is violated. On the other hand, the maximum radius of droplets on the vertical tube is constant for all peripheral angles and is smaller than other inclination.

The variation of heat flux with respect to subcooling temperature at different inclinations is shown in Fig. 15. The heat flux increases as subcooling or inclination increases. This behavior can be interpreted by considering the variation of the maximum droplet radius. According to Fig. 14, the maximum radius increases as inclination decreases.

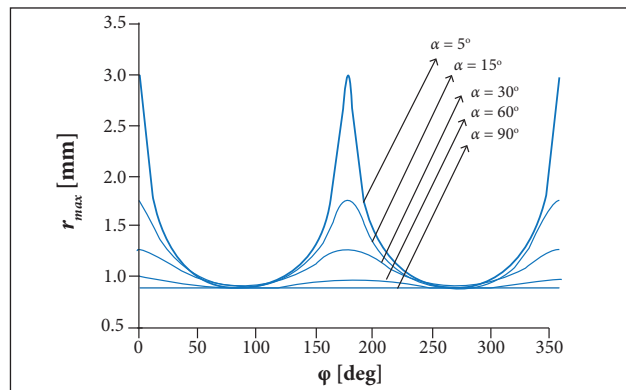


Figure 14. Variation of maximum droplet for peripheral angle at various inclinations.

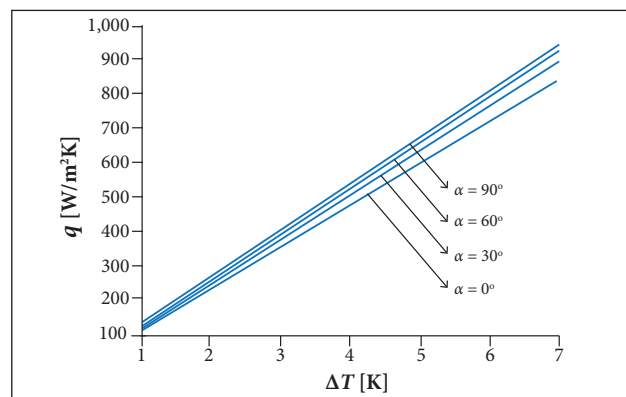


Figure 15. Variation of heat flux for surface subcooling at various inclinations of the tubes.

TOTAL BEHAVIOR OF DROPWISE CONDENSATION

The variation of heat flux with respect to subcooling temperature at various inclination of tube is shown in Fig. 15,

where $N_s = 10^{12}$ (1/m²), $\Delta\theta = 10^\circ$, and $\theta = 120^\circ$. Due to better sweep mechanism of vertical tube, the case of $\alpha = 90^\circ$ has the maximum heat flux. This result can be more cleared by comparing filmwise condensation and dropwise condensation behaviors. The heat transfer coefficient in filmwise condensation inversely depends on the condensate thickness, which is directly affected by the surface length. It means that higher condensate thickness leads to lower heat transfer coefficient in the case of filmwise condensation. Hence, horizontal tubes are employed in all shell and tube heat exchanger working in filmwise condensation. On the other hand, heat transfer coefficient of dropwise condensation is independent of the location and is uniform over the surface. These advantages indicate that vertical tubes can be used in heat exchangers working with dropwise condensation without any restriction in length.

The variation of heat flux with respect to contact angle is depicted in Fig. 16, where $N_s = 10^{12}$ (1/m²), $\Delta\theta = 10^\circ$, and $\Delta T = 5$ K. The contact angle has a significant effect on heat flux so that increasing contact angle from 100° to 160° nearly decreases q'' to $\frac{1}{3}$. Increasing contact angle results in higher thermal resistances (see Fig. 7), which leads to lower heat flux. It is worth mentioning that high contact angle usually couples with low contact angle hysteresis. Effect of contact angle hysteresis on the heat flux is given in Fig. 17, where $N_s = 10^{12}$ (1/m²), $\theta = 120^\circ$, and $\Delta T = 5$ K. Contact angle hysteresis has a considerable influence on the maximum radius. Increasing contact angle hysteresis leads to rapid decrease in the maximum radius, meaning that droplets with smaller radii slide quickly, off the surface and new droplets nucleate. Consequently, more small droplets population causes higher heat flux (according to Fig. 6).

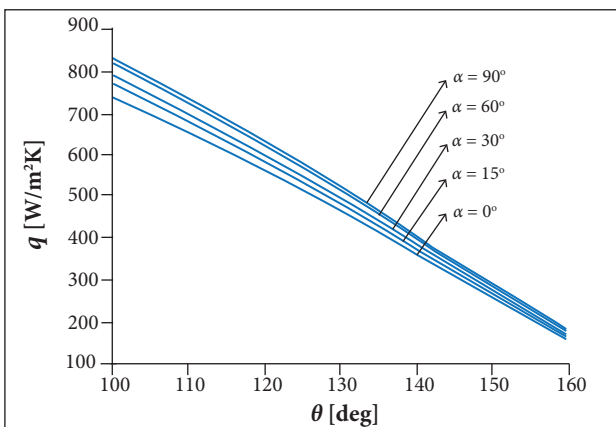


Figure 16. Variation of heat flux for contact angle at various inclinations of the tubes.

Figure 18 shows the effect of nucleation site number on the predicted dropwise condensation heat flux in a horizontal tube, where $\Delta\theta = 10^\circ$, $\theta = 120^\circ$, and $\alpha = 0^\circ$. The dropwise condensation heat flux increases with N_s . This outcome is explained by considering Fig. 10, where the nucleation site number has notable effect on the droplet population. Higher nucleation site number leads to greater droplet population and consequently higher total heat flux.

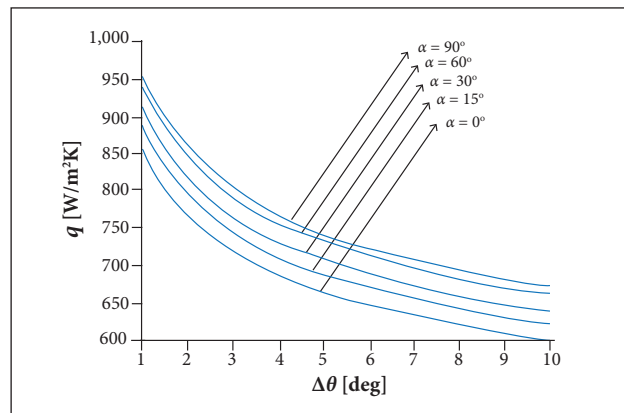


Figure 17. Variation of heat flux for contact angle hysteresis at various inclinations of the tubes.

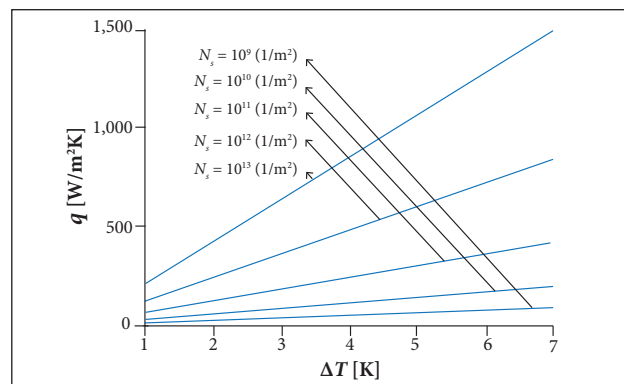


Figure 18. Variation of heat flux for surface subcooling at various nucleation sites.

CONCLUSION

An analytical model for calculation of dropwise condensation heat transfer on an inclined tube is presented. The results showed that heat transfer of vertical tubes is higher than other inclinations. This finding indicates that vertical tube must be used in shell and tube heat exchangers working in dropwise condition. On the other hand, the

current study, unlike the one of Hosokawa *et al.* (1995), indicates that increasing inclination enhances heat transfer in dropwise condensation on circular tubes. The reason is that a sliding droplet on more inclined tubes sweeps more droplets in their way. Therefore, further bare surface contacts with the vapor and heat transfer is enhanced.

REFERENCES

- Abu-Orabi M (1998) Modeling of heat transfer in dropwise condensation. *Int J Heat Mass Tran* 41(1):81-87. doi: 10.1016/S0017-9310(97)00094-X
- Battoo NK, Sikarwar BS, Khandekar S, Muralidhar K (2010) Mathematical modeling and simulation of dropwise condensation and inclined surfaces exposed to vapor flux. Proceedings of the 20th National and 9th International ISHMT-ASME Heat and Mass Transfer Conference; Mumbai, India.
- Carey VP (2007) *Liquid vapor phase change phenomena: an introduction to the thermophysics of vaporization and condensation processes in heat transfer equipment*. 2nd edition. Boca Raton: CRC Press.
- Cheng K, Kim S, Lee S, Kim KJ (2015) Internal dropwise condensation: modeling and experimental framework for horizontal tube condensers. *Int J Heat Mass Tran* 83:99-108. doi: 10.1016/j.ijheatmasstransfer.2014.11.084
- Citakoglu E, Rose JW (1969) Dropwise condensation — the effect of surface inclination. *Int J Heat Mass Tran* 12(5):645-650. doi: 10.1016/0017-9310(69)90045-3
- Dimitrakopoulos P, Higdon JJJ (1999) On the gravitational displacement of three-dimensional fluid droplets from inclined solid surfaces. *J Fluid Mech* 395:181-209. doi: 10.1017/S0022112099005844
- Dussan EB (1985) On the ability of drops or bubbles to stick to non-horizontal surfaces of solids. Part 2. Small drops or bubbles having contact angles of arbitrary size. *J Fluid Mech* 151:1-20. doi: 10.1017/S0022112085000842
- ElSherbini AI, Jacobi AM (2004) Liquid drops on vertical and inclined surfaces: II. A method for approximating drop shapes. *J Colloid Interface Sci* 273(2):566-575. doi: 10.1016/j.jcis.2003.12.043
- ElSherbini AI, Jacobi AM (2006) Retention forces and contact angles for critical liquid drops on non-horizontal surfaces. *J Colloid Interface Sci* 299(2):841-849. doi: 10.1016/j.jcis.2006.02.018
- Enright R, Miljkovic N, Alvarado JL, Kim K, Rose JW (2014) Dropwise condensation on micro- and nanostructured surfaces. *Nanoscale and Microscale Thermophysical Engineering* 18(3):223-250. doi: 10.1080/15567265.2013.862889
- Fayazbakhsh MA, Bahrami M (2013) Analytical modeling of mist condensation by natural convection over inclined flat surfaces. Proceedings of the ASME 2013 Heat Transfer Summer Conference collocated with the ASME 2013 7th International Conference on Energy Sustainability and the ASME 2013 11th International Conference on Fuel Cell Science, Engineering and Technology; Minneapolis, USA.

AUTHOR'S CONTRIBUTION

Conceptualization, Funding Acquisition, Resources, and Supervision, Saffari H; Methodology and Writing – Review & Editing, Saffari H and Bahrami HRT; Investigation, Simulation, and Writing – Original Draft, Bahrami HRT.

Glicksman LR, Hunt AW (1972) Numerical simulation of dropwise condensation. *Int J Heat Mass Tran* 15(11):2251-2269. doi: 10.1016/0017-9310(72)90046-4

Goncalves E, Houdeville R (2003) Numerical simulation of shock oscillations over airfoil using a wall law approach. *AIAA J* 41:1829-1832. doi: 10.2514/2.7303

Hosokawa T, Fujiwara Y, Ogami Y, Kawasima Y, Yamasaki Y (1995) Heat transfer characteristic of dropwise condensation on an inclined circular tube. *Heat Recovery Systems and CHP* 15(1):31-39. doi: 10.1016/0890-4332(95)90035-7

Hu HW, Tang GH (2014) Theoretical investigation of stable dropwise condensation heat transfer on a horizontal tube. *Appl Therm Eng* 62(2):671-679. doi: 10.1016/j.applthermaleng.2013.10.022

Ji T, Liebenberg L, Meyer JP (2009) Heat transfer enhancement during condensation in smooth tubes with helical wire inserts. *Heat Tran Eng* 30(5):337-352. doi: 10.1080/0145763080214466

Kananeh AB, Rausch MH, Leipertz A, Fröba AP (2010) Dropwise condensation heat transfer on plasma-ion-implanted small horizontal tube bundles. *Heat Tran Eng* 31(10):821-828. doi: 10.1080/01457630903547545

Kim HY, Lee HJ, Kang BH (2002) Sliding of liquid drops down an inclined solid surface. *J Colloid Interface Sci* 247(2):372-380. doi: 10.1006/jcis.2001.8156

Kim S, Kim KJ (2011) Dropwise condensation modeling suitable for superhydrophobic surfaces. *J Heat Transfer* 133(8):081502. doi: 10.1115/1.4003742

Kumar DS, Yuvaraj R (2013) Simulation of dropwise condensation on a superhydrophobic inclined substrate. Proceedings of the IEEE International Conference on Energy Efficient Technologies for Sustainability (ICEETS); Nagercoil, India.

Lee S, Yoon HK, Kim KJ, Kim S, Kennedy M, Zhang BJ (2013) A dropwise condensation model using a nano-scale, pin structured surface. *Int J Heat Mass Tran* 60:664-671. doi: 10.1016/j.ijheatmasstransfer.2013.01.032

LeFevre EJ, Rose JW (1966) A theory of heat transfer by dropwise condensation. In: *American Institute of Chemical Engineers. Chemical Engineering Progress Symposium Series*. 69 – 74 editions. New York: American Institute of Chemical Engineers.

Leipertz A, Fröba AP (2008) Improvement of condensation heat transfer by surface modifications. *Heat Tran Eng* 29(4):343-356. doi: 10.1080/01457630701821563

- Liu X, Cheng P (2015a) Dropwise condensation theory revisited: Part I. Droplet nucleation radius. *Int J Heat Mass Tran* 83:833-841. doi: 10.1016/j.ijheatmasstransfer.2014.11.009
- Liu X, Cheng P (2015b) Dropwise condensation theory revisited: Part II. Droplet nucleation density and condensation heat flux. *Int J Heat Mass Tran* 83:842-849. doi: 10.1016/j.ijheatmasstransfer.2014.11.008
- Maa JR (1978) Drop size distribution and heat flux of dropwise condensation. *Chem Eng J* 16(3):171-176. doi: 10.1016/0300-9467(78)85052-7
- McCormick JL, Westwater JW (1965) Nucleation sites for dropwise condensation. *Chem Eng Sci* 20(12):1021-1036. doi: 10.1016/0009-2509(65)80104-X
- McNeil DA, Burnside BM, Cuthbertson G (2000) Dropwise condensation of steam on a small tube bundle at turbine condenser conditions. *Experimental Heat Transfer* 13(2):89-105. doi: 10.1080/089161500269481
- Miljkovic N, Enright R, Wang EN (2012) Growth dynamics during dropwise condensation on nanostructured superhydrophobic surfaces. *Proceedings of the 3rd International Conference on Micro/Nanoscale Heat and Mass Transfer*. American Society of Mechanical Engineers; Atlanta, USA.
- Miljkovic N, Wang EN (2013) Condensation heat transfer on superhydrophobic surfaces. *MRS Bulletin* 38(5):397-406. doi: 10.1557/mrs.2013.103
- Mu C, Pang J, Lu Q, Liu T (2008) Effects of surface topography of material on nucleation site density of dropwise condensation. *Chem Eng Sci* 63(4):874-880. doi: 10.1016/j.ces.2007.10.016
- O'Callaghan PW, Babus'Haq RF (1990) Cooling problems facing the electronics and aerospace industries. *Aircraft Engineering and Aerospace Technology* 62(7):17-19. doi: 10.1108/eb036968
- Palen JW, Breber G, Taborek J (1979) Prediction of flow regimes in horizontal tube-side condensation. *Heat Tran Eng* 1(2):47-57. doi: 10.1080/01457637908939558
- Peng B, Ma X, Lan Z, Xu W, Wen R (2015) Experimental investigation on steam condensation heat transfer enhancement with vertically patterned hydrophobic-hydrophilic hybrid surfaces. *Int J Heat Mass Tran* 83:27-38. doi: 10.1016/j.ijheatmasstransfer.2014.11.069
- Preston DJ (2014) Electrostatic charging of jumping droplets on superhydrophobic nanostructured surfaces: fundamental study and applications (Master's thesis). Cambridge: Massachusetts Institute of Technology.
- Reis FMM, Lavielle P, Miscevic M (2016) Dropwise condensation enhancement using a wettability gradient. *Heat Tran Eng* 38(3):377-385. doi: 10.1080/01457632.2016.1189277
- Rohsenow WM (1972) Status of and problems in boiling and condensation heat transfer. In: Hetsroni G, Sideman S, Hartnett JP, editors. *Progress in heat and mass transfer*. Vol. 6: Proceedings of the International Symposium on Two-phase Systems. Oxford: Pergamon Press.
- Rose JW (2002) Dropwise condensation theory and experiment: a review. *Proc IME J Power Energ* 216(2):115-128. doi: 10.1243/09576500260049034
- Schmidt E, Schurig W, Sellschopp W (1930) Versuche über die Kondensation von Wasserdampf in Film- und Tropfenform. *Technische Mechanik und Thermodynamik* 1(2):53-63.
- Schrage RW (1953) *A theoretical study of interphase mass transfer*. New York: Columbia University Press.
- Sikarwar BS, Battoo NK, Khandekar S, Muralidhar K (2011) Dropwise condensation underneath chemically textured surfaces: simulation and experiments. *J Heat Transfer* 133(2):021501. doi: 10.1115/1.4002396
- Sikarwar BS, Khandekar S, Agrawal S, Kumar S, Muralidhar K (2012) Dropwise condensation studies on multiple scales. *Heat Tran Eng* 33(4-5):301-341. doi: 10.1080/01457632.2012.611463
- Sikarwar BS, Muralidhar K, Khandekar S (2013) Effect of drop shape on heat transfer during dropwise condensation underneath inclined surfaces. *Interfacial Phenomena and Heat Transfer* 1(4):339-356. doi: 10.1615/InterfacPhenomHeatTransfer.v1.i4.30
- Sun FZ, Gao M, Lei SH, Zhao YB, Wang K, Shi YT, Wang NH (2007) The fractal dimension of the fractal model of dropwise condensation and its experimental study. *International Journal of Nonlinear Sciences and Numerical Simulation* 8(2):211-222. doi: 10.1515/IJNSNS.2007.8.2.211
- Talesh Bahrami HR, Ahmadi B, Saffari H (2017) Optimal condition for fabricating superhydrophobic copper surfaces with controlled oxidation and modification processes. *Mater Lett* 189:62-65. doi: 10.1016/j.matlet.2016.11.076
- Tanaka H (1975) A theoretical study of dropwise condensation. *J Heat Transfer* 97(1):72-78. doi: 10.1115/1.3450291
- Tanasawa I (1991) Advances in condensation heat transfer. *Advances in Heat Transfer* 21:55-139. doi: 10.1016/S0065-2717(08)70334-4
- Thome JR (2015) *Encyclopedia of two-phase heat transfer and flow I: fundamentals and methods*. Vol. 2. New Jersey: World Scientific.
- Vemuri S, Kim KJ (2006) An experimental and theoretical study on the concept of dropwise condensation. *Int J Heat Mass Tran* 49(3-4):649-657. doi: 10.1016/j.ijheatmasstransfer.2005.08.016
- Wen HW, Jer RM (1976) On the heat transfer in dropwise condensation. *The chemical engineering journal* 12(3):225-231. doi: 10.1016/0300-9467(76)87016-5
- Wu YT, Yang CX, Yuan XG (2001) Drop distributions and numerical simulation of dropwise condensation heat transfer. *Int J Heat Mass Tran* 44(23):4455-4464. doi: 10.1016/S0017-9310(01)00085-0
- Yamamoto S (2003) Onset of condensation in vortical flow over sharp-edged delta wing. *AIAA J* 41(9):1832-1835. doi: 10.2514/2.7304
- Yun BY, No HC, Shin CW (2016) Modeling of high pressure steam condensation in inclined horizontal tubes of PAFS in APR+. *J Nucl Sci Tech* 53(9):1353-1365. doi: 10.1080/00223131.2015.1110505